Long-time coherence in echo spectroscopy with $\pi/2$-π-$\pi/2$ pulse sequence

Arseni Goussev
School of Mathematics, University of Bristol, University Walk, Bristol BS8 1TW, United Kingdom

Philippe Jacquod
Physics Department, University of Arizona, 1118 East 4th Street, Tucson, Arizona 85721, USA

(Received 2 June 2010; published 18 November 2010)

Motivated by atomic optics experiments, we investigate a class of fidelity functions describing the reconstruction of quantum states by time-reversal operations as $M_{\rm Da}(t) = |\langle\psi|e^{iH_2t/2}e^{iH_1t/2}e^{-iH_2t/2}e^{-iH_1t/2}|\psi\rangle|^2$. We show that the decay of $M_{\rm Da}$ is quartic in time at short times and that it freezes well above the ergodic value at long times, when H_2-H_1 is not too large. The long-time saturation value of $M_{\rm Da}$ contains easily extractable information on the strength of decoherence in these systems.

DOI: 10.1103/PhysRevA.82.052114 PACS number(s): 03.65.Yz, 05.45.Mt

I. INTRODUCTION

When subjected to external noisy fields, quantum-mechanical wave functions lose memory of their phase. As a fundamentally important consequence of this *decoherence* process, pairs of partially scattered waves no longer interfere, and the dynamics follows the Liouville time evolution of classical densities [1]. A somehow similar situation occurs when one evolves an initial superposition $\phi = \sum_\alpha c_\alpha \psi_\alpha$ of many eigenmodes ψ_α of the Hamiltonian H_1 governing the time evolution, with incommensurate eigenfrequencies ϵ_α. In this case, for each pair of components (α,β), the relative phase $(\epsilon_\alpha - \epsilon_\beta)t$ becomes pseudorandom, which washes out partial-wave interferences. This *dephasing* process, however, differs from decoherence in a fundamental way in that it can, in principle, be undone by an appropriate time inversion. As a matter of fact, echo experiments are able to reverse the sign of the Hamiltonian, $H_1 \to -H_1$, by means of effective changes of coordinate axes induced by electromagnetic pulses [2]. When this operation is performed after an evolution time t, one expects the initial wave function to be reconstructed at $2t$, regardless of its spread over eigenmodes. Imperfections in the pulse sequence or unavoidable couplings to external uncontrolled degrees of freedom result instead in an imperfect time inversion, $H_1 \to -H_2 = -H_1 - \Sigma$, and therefore the Loschmidt echo [3–7] (we set $\hbar \equiv 1$),

$$M_{\rm L}(t) = |m_{\rm L}(t)|^2, \quad \text{with} \tag{1a}$$

$$m_{\rm L}(t) = \langle\psi|e^{iH_2t}e^{-iH_1t}|\psi\rangle, \tag{1b}$$

gives a better description of the fidelity with which the experiment reconstructs the initial state. Echo experiments in nuclear magnetic resonance [2,8], quantum optics [9], atoms [10–12], condensed matter [13], microwave cavities [14], and elastodynamics [15] have demonstrated that $M_{\rm L}(t)$ remains sizable for times significantly longer than the dephasing time. The decay of $M_{\rm L}(t)$ allows one to extract information on irreversible decoherence processes induced by Σ.

In experiments with cold atoms, the Loschmidt echo, $M_{\rm L}$, can be extracted from interference fringes of Ramsey spectroscopy [16]. There, an effectively two-level atom is initially prepared in a state $|1\rangle \otimes |\psi\rangle$, where $|1\rangle$ and $|2\rangle$ denote the two internal atomic states and $|\psi\rangle$ stands for the spatial component of the initial state. First, the atom is irradiated with a microwave frequency field with energy chosen to change the atomic state into an equiprobable superposition of $|1\rangle \otimes |\psi\rangle$ and $|2\rangle \otimes |\psi\rangle$. Such a field is referred to as a $\pi/2$ pulse. The atom is then let to evolve in an optical trap for a time t, during which the $|1\rangle$ component of the state evolves under a spatial Hamiltonian H_1, while the $|2\rangle$ component under H_2. After that, another $\pi/2$ pulse is applied to the atom and the probability P_2 of the atom being found in the internal state $|2\rangle$ is measured. It turns out that this probability is essentially determined by the Loschmidt echo amplitude, $m_{\rm L}$. In practice, however, one works not with a pure initial state $|\psi\rangle$, but with a thermal mixture of initial states. The echo amplitude $m_{\rm L}$ from each of these states contributes to P_2 with a different, effectively random phase, which in turn reduces the fringe contrast in a Ramsey experiment. As a result, the $\pi/2$-$\pi/2$ pulse sequence proves inefficient in measuring the Loschmidt echo for large ensembles of thermally populated states.

In order to overcome this difficulty, Davidson and collaborators implemented a pulse sequence in their echo spectroscopy experiments [11,12]:

$$M_{\rm Da}(t) = |m_{\rm Da}(t)|^2, \quad \text{with} \tag{2a}$$

$$m_{\rm Da}(t) = \langle\psi|e^{iH_2t/2}e^{iH_1t/2}e^{-iH_2t/2}e^{-iH_1t/2}|\psi\rangle. \tag{2b}$$

The corresponding pulse sequence consisted of three short pulses, $\pi/2$-π-$\pi/2$, separated by two time intervals of equal duration $t/2$, after which P_2 was measured. The π pulse swaps the population of the internal states $|1\rangle$ and $|2\rangle$. The probability P_2 is then determined by the amplitude $m_{\rm Da}$, and each individual state of the thermal ensemble contributes to P_2 with the same phase. Thus, the $\pi/2$-π-$\pi/2$ pulse sequence allows one to measure the echo in Eq. (2) even for ensembles of more than 10^6 of thermally populated states, as in the experiments of Refs. [11,12].

It is clear from the definitions given by Eqs. (1) and (2) that, mathematically, $M_{\rm Da}$ is not the same quantity as the Loschmidt echo $M_{\rm L}$. Even though some significant differences between $M_{\rm Da}$ and $M_{\rm L}$ have been previously envisaged in the literature, they have never been systematically studied. It is the purpose of this article to fill this gap by comparing the two

quantities both analytically and numerically. In what follows, we show that $M_{\rm Da}$ differs from the Loschmidt echo $M_{\rm L}$ in the two important respects that (i) its short-time decay is quartic and not quadratic in time and (ii) for not too strong perturbation $\Sigma = H_2 - H_1$, $M_{\rm Da}$ saturates at a perturbation-dependent value, well above the ergodic saturation of $M_{\rm L}(\infty) \sim N^{-1}$ at the inverse Hilbert space size. Fidelity freezes have been reported for Loschmidt echoes with off-diagonal perturbations with a zero time average [17], phase-space displacement perturbations [18], and more recently for initially pure states coupled to complex environments [19]; however, the freeze we report here has a different physical origin. We note in particular that it persists for $t \to \infty$. The long-time saturation of $M_{\rm Da}$ makes it possible to extract the strength of the fields in Σ more easily than by fitting decay curves of conventional echoes over not precisely defined time intervals. Moreover, the absence of decay arising from Σ in this pulse sequence makes it straightforward to extract decoherence rates because, assuming that the pulse sequence is perfect, any decay in experimentally obtained data for $M_{\rm Da}(t)$ would come exclusively from the coupling of the system to external degrees of freedom, not included in our theory. Given the superb experimental control that modern echo experiments have on their pulse sequence, this echo spectroscopy has therefore the potential to deliver precious, previously unattainable information on the dominant sources of decoherence in trapped cold atomic gases.

II. SHORT-TIME DECAY

There has been a large number of analytical and numerical investigations of the Loschmidt echo and some of its offspring [3,4]. Most, if not all approaches assume a small perturbation; that is, $|\Sigma| \ll |H_{1,2}|$ for an appropriate operator norm. As but one consequence, the largest energy scale is the energy bandwidth B, which to leading order is the same for H_1 and H_2. For short times, $t \ll B^{-1}$, $M_{\rm L}(t)$ is easily calculated by expanding the propagators in Eqs. (1) and keeping the leading-order contributions. One obtains

$$M_{\rm L}(t) \simeq 1 - (\sigma_{\rm L} t)^2, \tag{3}$$

where

$$\sigma_{\rm L}^2 = \langle\psi|\Sigma_{\rm L}^2|\psi\rangle - \langle\psi|\Sigma_{\rm L}|\psi\rangle^2, \quad \Sigma_{\rm L} = H_1 - H_2. \tag{4}$$

Thus, the short-time decay of the Loschmidt echo is *quadratic* [5,6], with a rate given by the dispersion $\sigma_{\rm L}$ of the perturbation operator $\Sigma_{\rm L}$ evaluated over the initial state.

The same procedure can be applied to $M_{\rm Da}$, where it, however, gives

$$M_{\rm Da}(t) \simeq 1 - (\sigma_{\rm Da} t)^4, \tag{5}$$

with the decay rate $\sigma_{\rm Da}$ given by

$$\sigma_{\rm Da}^4 = \langle\psi|\Sigma_{\rm Da}^2|\psi\rangle - \langle\psi|\Sigma_{\rm Da}|\psi\rangle^2, \quad \Sigma_{\rm Da} = \frac{i}{4}[H_1, H_2]. \tag{6}$$

Two things are remarkable here. First, the short-time decay of $M_{\rm Da}$ is *quartic* in t and thus slower than the decay of $M_{\rm L}$. Second, its rate is determined by the *commutator* of the unperturbed and perturbed Hamiltonians.

III. LONG-TIME SATURATION

The analysis of the long-time behavior of $M_{\rm L}$ and $M_{\rm Da}$ starts by diagonalizing the unperturbed and perturbed Hamiltonian operators, $H_1 = \sum_u E_u|u\rangle\langle u|$ and $H_2 = \sum_v E_v|v\rangle\langle v|$, respectively, and expanding the initial state on the basis of the unperturbed Hamiltonian, $|\psi\rangle = \sum_u c_u|u\rangle$ [4]. The resulting expression for the echo is then averaged over time to yield the mean saturation value. In the case of the Loschmidt echo the time-averaged saturation is given by

$$M_{\rm L,\infty} = \sum_{u,u',u'',v} c_u^* c_{u''} |c_{u'}|^2 \langle u|v\rangle\langle v|u'\rangle\langle u'|v\rangle\langle v|u''\rangle. \tag{7}$$

The next step is to average this expression over a random ensemble of coefficient c_u for the initial state such that $\overline{c_u^* c_{u'}} = N^{-1}\delta_{u,u'}$. (Hereinafter, an overline denotes the averaging over an ensemble of random initial states.) Here N is the effective size of the Hilbert space (the number of eigenstates of $H_{1,2}$ comprising the initial state). To leading order in $1/N$, one uses $\overline{c_u^* c_{u''}|c_{u'}|^2} = \overline{c_u^* c_{u''}|c_{u'}|^2} = N^{-2}\delta_{u,u''}$ to obtain the ergodic saturation value

$$\overline{M_{\rm L,\infty}} = \frac{1}{N}. \tag{8}$$

Using the same procedure, one can calculate the long-time saturation value of $M_{\rm Da}$. At the level of the echo amplitude $m_{\rm Da}$, one gets

$$\overline{m_{\rm Da,\infty}} = \sum_{u,u',v} \overline{c_u^* c_{u'}} \langle u|v\rangle\langle v|u'\rangle\langle u'|v\rangle\langle v|u'\rangle \tag{9a}$$

$$= \frac{1}{N}\sum_{u,v} |\langle u|v\rangle|^4. \tag{9b}$$

One then uses an approximation $\overline{|\langle u|v\rangle|^4} \simeq \overline{|\langle u|v\rangle|^2}^2$ with $\overline{|\langle u|v\rangle|^2} = \rho(E_u - E_v)$ a function of only the energy difference between the two states. Replacing one of the sums in Eq. (9) by an integral over the energy difference between the two states scaled by the mean level spacing $\Delta = B/N$, we can write

$$\overline{m_{\rm Da,\infty}} \simeq \int \frac{dE}{\Delta}\rho^2(E). \tag{10}$$

This expression relates the long-time saturation of $M_{\rm Da}$ to the energy spreading of eigenfunctions of H_1 over those of H_2 as measured by $\rho(E)$. It is known for a large variety of quantum chaotic systems that, in the regime $\Delta \ll \Gamma/\Delta \ll B$, this spreading has a Lorentzian shape,

$$\rho(E_u - E_v) \simeq \frac{\Delta}{\pi}\frac{\Gamma/2}{(E_u - E_v)^2 + (\Gamma/2)^2}, \tag{11}$$

with a spreading width given by the golden rule, $\Gamma \simeq \sigma_{\rm L}^2/\Delta$ [20]; see Eq. (4) for the definition of $\sigma_{\rm L}^2$. We thus obtain

$$\overline{m_{\rm Da,\infty}} \simeq \frac{\Delta}{\pi\Gamma}. \tag{12}$$

Equations (11) and (12) predict an average saturation value $\overline{M_{\rm Da,\infty}}$ above the ergodic saturation for $N < (B/\pi\Gamma)^2$. The

width Γ of the Lorentzian (11) increases with $|\Sigma|$, and the ergodic saturation [Eq. (8)] is recovered when $\Gamma > B/\pi N^{1/2}$; thus,

$$\overline{M_{\mathrm{Da},\infty}} \simeq \max\left[\left(\frac{\Delta}{\pi\Gamma}\right)^2, \frac{1}{N}\right]. \tag{13}$$

We note that the Lorentzian spreading of Eq. (11) is replaced by more complicated, system-dependent spiked structures in dynamical systems with mixed or regular dynamics, for which it is accordingly impossible to draw general conclusions. We stress, however, that Eq. (10) remains valid even in that case.

Equation (13) is the main result of this article. This new long-time fidelity saturation originates from the specific sequence of time evolutions in M_{Da}, giving the long-time behavior of the latter as an energy integral over the *squared* average overlap $|\langle u|v\rangle|^4$ of eigenstates $|u\rangle$ of H_1 over the eigenstates $|v\rangle$ of H_2. For completeness we next comment on the intermediate regime, between the short-time quartic decay and the long-time saturation.

IV. INTERMEDIATE ASYMPTOTIC DECAY

We briefly sketch a semiclassical analysis of M_{Da} in the intermediate regime between the short-time decay and the long-time saturation. We follow the lines of Ref. [7] to show that M_{Da} and M_{L} have the same behavior in that regime.

In the semiclassical approximation the time evolution of $|\psi\rangle$ under H_j, $j = 1,2$, is given by

$$\langle \mathbf{r}|e^{-iH_j t}|\psi\rangle = \int d\mathbf{r}' \sum_{\gamma(\mathbf{r}'\to\mathbf{r},t)} D_{j,\gamma}\, e^{iS_{j,\gamma}} \langle \mathbf{r}'|\psi\rangle. \tag{14}$$

Here the sum goes over all classical paths γ connecting $\mathbf{r}'$ and $\mathbf{r}$ in time t, $S_{j,\gamma} = S_{j,\gamma}(\mathbf{r},\mathbf{r}',t)$ is the action along γ, $D_{j,\gamma} = (2\pi i)^{-d/2}|\det(\partial^2 S_{j,\gamma}/\partial\mathbf{r}\partial\mathbf{r}')|^{1/2} e^{-i\pi\nu_{j,\gamma}/2}$ with Morse index $\nu_{j,\gamma}$ counting the number of conjugate points on γ, and d is the dimensionality of the system [21]. The semiclassical Loschmidt echo amplitude is obtained by inserting Eq. (14) into Eq. (1b). The resulting expression contains three spatial integrals over $\mathbf{r}$, $\mathbf{r}'$, and $\mathbf{r}''$ with a double sum over trajectories $\gamma_1(\mathbf{r}' \to \mathbf{r},t)$ and $\gamma_2(\mathbf{r}'' \to \mathbf{r},t)$ corresponding to the Hamiltonians H_1 and H_2, respectively. The standard analysis of this expression involves three steps [7]. (i) One assumes that $\langle \mathbf{r}|\psi\rangle$ is localized about a point $\mathbf{r}_0$ and evaluates the integrals over $\mathbf{r}'$ and $\mathbf{r}''$ using stationary phase approximations. This reduces the set of paths γ_1 and γ_2 to those starting at $\mathbf{r}_0$ (see Fig. 1). (ii) Noting that the double sum over trajectories contains rapidly oscillating phase factors $\exp[i(S_{1,\gamma_1} - S_{2,\gamma_2})]$, so that only pairs of correlated paths γ_1 and γ_2 contribute to m_{Da}, one employs the diagonal approximation ($\gamma_2 \simeq \gamma_1$) to reduce m_{L} to a sum over a single path γ_1. Reference [22], building on ideas first expressed in Ref. [6], justified this step using the shadowing theorem. (iii) Finally, one uses the fact that $|D_{1,\gamma_1}|^2$ is the Jacobian of a transformation between final positions $\mathbf{r}$ and initial momenta $\mathbf{p}$ on paths γ_1. This allows one to change the integration variable from $\mathbf{r}$ to $\mathbf{p}$ to get

$$m_{\mathrm{L}}(t) = (2\pi)^{-d} \int d\mathbf{p}\, e^{i\Delta S} |\langle \mathbf{p}|\psi\rangle|^2. \tag{15}$$

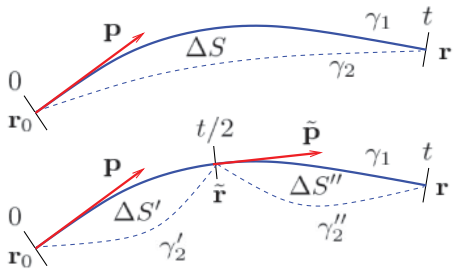

FIG. 1. (Color online) Trajectories of the unperturbed (γ_1) and perturbed (γ_2, γ_2', and γ_2'') systems together with the associated action differences (ΔS, $\Delta S'$, and $\Delta S''$).

Here $\Delta S = \Delta S(\mathbf{r}_0,\mathbf{p},t) = S_{1,\gamma_1} - S_{2,\gamma_2}$ is the difference between the action of an unperturbed trajectory γ_1 leaving the point $\mathbf{r}_0$ with a momentum $\mathbf{p}$ and traveling for time t and the action of the corresponding perturbed trajectory $\gamma_2 \simeq \gamma_1$. Following the same procedure, one finds

$$m_{\mathrm{Da}}(t) = (2\pi)^{-d} \int d\mathbf{p}\, e^{i(\Delta S' - \Delta S'')} |\langle \mathbf{p}|\psi\rangle|^2, \tag{16}$$

where $\Delta S' = \Delta S(\mathbf{r}_0,\mathbf{p},t/2)$ and $\Delta S'' = \Delta S(\tilde{\mathbf{r}},\tilde{\mathbf{p}},t/2)$, with $(\tilde{\mathbf{r}},\tilde{\mathbf{p}})$ being the phase-space point on γ_1 at time $t/2$ (see Fig. 1). In other words, $\Delta S'$ ($\Delta S''$) is the action difference between the first (second) half of the unperturbed trajectory γ_1 and the corresponding perturbed trajectory γ_2' (γ_2''). This is sketched in Fig. 1.

Once averaged over an ensemble of initial states, both M_{L} and M_{Da} satisfy

$$\overline{M_{\mathrm{L,Da}}(t)} \simeq \overline{m_{\mathrm{L,Da}}(t)}^2 + (2\pi)^{-2d} \int d\mathbf{p} \int_{\Omega_{\mathbf{p}}} d\mathbf{p}'\, |\langle \mathbf{p}|\psi\rangle|^2\, |\langle \mathbf{p}'|\psi\rangle|^2, \tag{17}$$

where the integral over $\mathbf{p}'$ is restricted to a volume $\Omega_{\mathbf{p}}$ around $\mathbf{p}$, such that two trajectories starting from the same spatial point with momenta $\mathbf{p}$ and $\mathbf{p}' \in \Omega_{\mathbf{p}}$ stay "close" in phase space during time t. The first term on the right-hand side of Eq. (17) is evaluated using the central limit theorem, $\overline{\exp(i\Delta S)} \simeq \exp(-\overline{\Delta S^2}/2) \simeq e^{-\Gamma t/2}$ and $\overline{\exp[i(\Delta S' - \Delta S'')]} \simeq \exp[-(\overline{\Delta S'^2} + \overline{\Delta S''^2})/2] \simeq e^{-\Gamma(t/2+t/2)/2} = e^{-\Gamma t/2}$, where Γ is defined in Eq. (11) as the width of the local density of states. For M_{Da}, we neglect correlations between $\Delta S'$ and $\Delta S''$, which is justified by the fast decay of correlations along chaotic classical trajectories. The second term in Eq. (17) is determined by the measure of the set $\Omega_{\mathbf{p}}$ and in chaotic systems decays as $e^{-\lambda t}$ with λ being the average Lyapunov exponent of the underlying classical system [7]. Therefore, the intermediate time decay of M_{Da} is the same as that of M_{L} [7,23], that is,

$$\overline{M_{\mathrm{L}}(t)} \simeq \overline{M_{\mathrm{Da}}(t)} \sim e^{-t\min[\Gamma,\lambda]}. \tag{18}$$

This exponential time decay continues until the echo reaches the saturation plateau given by Eq. (13).

Reference [11] reported some saturation of M_{Da} for ultracold atoms inside optical traps. However, at this stage, a direct comparison of these experiments with our theory does not seem feasible, because they explore completely

different time regimes. Indeed, the echo spectroscopy experiments of Refs. [11,12] are concerned with short times corresponding to no more than three to four oscillations or bounces of an atom in the trap. In contrast, the semiclassical derivation of the exponential decay [Eq. (18)] and the RMT analysis of the fidelity freeze [Eq. (13)] are only valid for times much longer than the average free-flight time.

V. NUMERICAL STUDY

We confirm our analytical results with some numerical data. Our simulations are based on the kicked rotator model with dimensionless Hamiltonian:

$$H_{1(2)} = \frac{\hat{p}^2}{2} + K_{1(2)} \cos \hat{x} \sum_n \delta(t - n\tau). \tag{19}$$

For large-enough kicking strength, $K_{1(2)}\tau > 7$, the dynamics is fully chaotic with a Lyapunov exponent $\lambda = \ln[K_{1(2)}\tau/2]$. We quantize this Hamiltonian on a torus and accordingly consider discrete values $p_l = 2\pi l/N$ and $x_l = 2\pi l/N$, $l = 1, \ldots, N$, giving an effective Planck's constant $\hbar_{\rm eff} = 1/N$. Both echoes $M_{\rm L}(n)$ and $M_{\rm Da}(n)$ are computed for discrete times $t = n\tau$, with the kicking period τ, using the unitary Floquet operators $U_{1(2)} = \exp[-i\hat{p}^2/2\hbar_{\rm eff}] \exp[-iK_{1(2)} \cos \hat{x}/\hbar_{\rm eff}]$ for single-kick time evolutions. The bandwidth is $B = 2\pi$ and, accordingly, $\Delta = 2\pi/N$. The eigenstates of U_2 spread over those of U_1 according to Eq. (11) with $\Gamma \propto (\delta K\, N)^2$, with $\delta K = K_2 - K_1$ [4]. Together with Eq. (13), we thus expect a long-time saturation of $M_{\rm Da}$ at a value

$$\overline{M_{{\rm Da},\infty}} \sim (\delta K^2 N^3)^{-2}, \tag{20}$$

for $\delta K^4 N^5 < 1$.

Figure 2 shows the time decay of the echoes, $\overline{M_{\rm L}(t)}$ shown as red curves and $\overline{M_{\rm Da}(t)}$ as black curves, averaged over

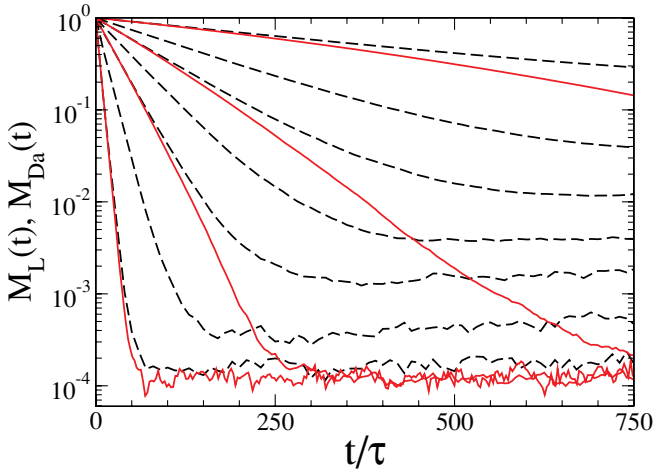

FIG. 2. (Color online) Average echo decay for the kicked rotator model with $K_1 = 57$, $N = 8192$, $K_2 - K_1 = 5 \times 10^{-5}$, 1.2×10^{-4}, 2.1×10^{-4}, and 5×10^{-4} ($M_{\rm L}$, red solid lines from top to bottom), and $K_2 - K_1 = 5 \times 10^{-5}$, 9×10^{-5}, 1.2×10^{-4}, 1.6×10^{-4}, 2.1×10^{-4}, 3.1×10^{-4}, and 5×10^{-4} ($M_{\rm Da}$, black dashed lines, from top to bottom). Curves are averages over 500 initial states.

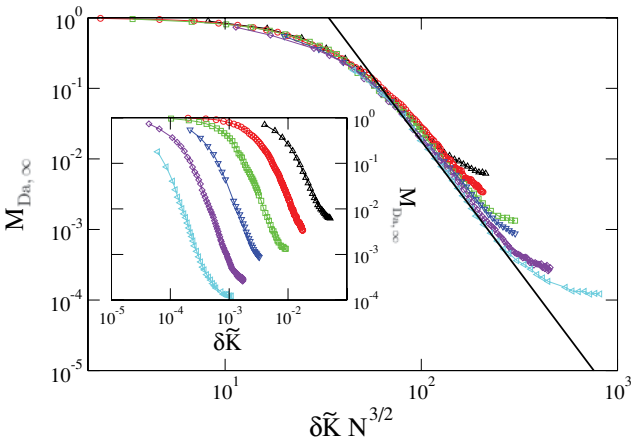

FIG. 3. (Color online) Long-time saturation value of $M_{\rm Da}$ for $K_1 = 57$ and $N = 256$ (black up-pointing triangles), 512 (red circles), 1024 (green squares), 2048 (blue down-pointing triangles), 4096 (violet diamonds), and 8192 (cyan left-pointing triangles). (Main panel) Rescaled data confirming the analytical prediction of Eq. (20). The straight black line indicates a slope of $\propto 1/x^{3.8}$. (Inset) Raw data as function of the difference of dimensionless kicking strengths $\delta\tilde{K} = \tilde{K}_2 - \tilde{K}_1$, with $\tilde{K}_{1(2)} = K_{1(2)}/\tau$.

an ensemble of randomly chosen initial states. For equal values of the perturbation strength, both $M_{\rm L}$ and $M_{\rm Da}$ display an exponential time decay governed by the same decay rate, providing a clear support for Eq. (18). The Loschmidt echo decay saturates at a value $\sim N^{-1}$, in agreement with Eq. (8). The freeze of $M_{\rm Da}$ occurs at a value that decreases with increasing perturbation strength until it reaches ergodic saturation at N^{-1}. We confirm in Fig. 3 that the numerically observed perturbation-dependent saturation of $M_{\rm Da}$ follows Eq. (20). Once plotted as a function of $\delta K N^{3/2}$, saturation data for $N \in [256,8192]$ and $\delta K \in [4 \times 10^{-5}, 0.052]$ nicely fall on top of one another until they deviate because they have different ergodic saturation, N^{-1}. Moreover, in the regime of validity $\Delta \ll \delta K \ll B$ of Eq. (11), one has $M_{{\rm Da},\infty} \propto (\delta K N^{3/2})^b$ with an exponent $b \simeq 3.8$ close to the prediction $b = 4$ from Eq. (20). We note that b is larger for data with larger Hilbert space size N, where the fitting range is larger—and the fit is accordingly more accurate—because saturation occurs at larger values of $\delta K N^{3/2}$. We also checked numerically that the initial decay of $M_{\rm Da}$ is quartic and not quadratic in time. Our numerical simulations thus fully confirm the theoretical predictions derived earlier.

VI. CONCLUSIONS

Our analysis of the fidelity function $M_{\rm Da}$ [11,12] shows that it significantly differs from the Loschmidt echo in two important respects: (i) The short-time decay of $M_{\rm Da}$ is quartic (and not quadratic) in time and is governed by the commutator (and not the difference) of the unperturbed and perturbed Hamiltonians, and (ii) for not too strong Hamiltonian perturbations, the decay of $M_{\rm Da}$ freezes at values inversely proportional to the square of the measure Γ of the perturbation, as defined by the width of the local density of states [Eq. (11)]. This makes it possible to estimate the strength of decoherence processes in systems of cold trapped

atoms by fitting the saturation value of M_{Da}, which is arguably easier and more precise than fitting decay curves over not precisely defined time intervals. In addition to providing an analytic derivation of this finding, in particular relating the saturation level to the strength of decoherence fields, and to predicting an initial quartic decay of M_{Da}, our theory gives an intermediate behavior of M_{Da} which follows that of the Loschmidt echo M_{L}. We confirmed these analytical findings numerically.

ACKNOWLEDGMENT

A.G. acknowledges the support of EPSRC under Grant No. EP/E024629/1.

[1] E. Joos, H. D. Zeh, C. Kiefer, D. Giulini, J. Kupsch, and I.-O. Stamatescu, *Decoherence and the Appearance of a Classical World in Quantum Theory* (Springer, Berlin, 2003).
[2] E. L. Hahn, Phys. Rev. **80**, 580 (1950).
[3] T. Gorin, T. Prosen, T. H. Seligman, and M. Znidaric, Phys. Rep. **435**, 33 (2006).
[4] Ph. Jacquod and C. Petitjean, Adv. Phys. **58**, 67 (2009).
[5] A. Peres, Phys. Rev. A **30**, 1610 (1984).
[6] N. R. Cerruti and S. Tomsovic, Phys. Rev. Lett. **88**, 054103 (2002).
[7] R. A. Jalabert and H. M. Pastawski, Phys. Rev. Lett. **86**, 2490 (2001); F. M. Cucchietti, H. M. Pastawski, and R. A. Jalabert, Phys. Rev. B **70**, 035311 (2004).
[8] S. Zhang, B. H. Meier, and R. R. Ernst, Phys. Rev. Lett. **69**, 2149 (1992).
[9] N. A. Kurnit, I. D. Abella, and S. R. Hartmann, Phys. Rev. Lett. **13**, 567 (1964).
[10] F. B. J. Buchkremer, R. Dumke, H. Levsen, G. Birkl, and W. Ertmer, Phys. Rev. Lett. **85**, 3121 (2000).
[11] M. F. Andersen, A. Kaplan, and N. Davidson, Phys. Rev. Lett. **90**, 023001 (2003).
[12] M. F. Andersen, T. Grünzweig, A. Kaplan, and N. Davidson, Phys. Rev. A **69**, 063413 (2004); M. F. Andersen, A. Kaplan, T. Grünzweig, and N. Davidson, Phys. Rev. Lett. **97**, 104102 (2006).
[13] Y. Nakamura, Yu. A. Pashkin, T. Yamamoto, and J. S. Tsai, Phys. Rev. Lett. **88**, 047901 (2002).
[14] R. Schäfer, H.-J. Stöckmann, T. Gorin, and T. H. Seligman, Phys. Rev. Lett. **95**, 184102 (2005); R. Schäfer, T. Gorin, T. H. Seligman, and H.-J. Stöckmann, New J. Phys. **7**, 152 (2005).
[15] T. Gorin, T. H. Seligman, and R. L. Weaver, Phys. Rev. E **73**, 015202(R) (2006); O. I. Lobkis and R. L. Weaver, *ibid.* **78**, 066212 (2008).
[16] See Refs. [11,12] for details on experimental techniques of Ramsey and echo spectroscopy.
[17] T. Prosen and M. Znidaric, New J. Phys. **5**, 109 (2003); Phys. Rev. Lett. **94**, 044101 (2005).
[18] C. Petitjean, D. V. Bevilaqua, E. J. Heller, and Ph. Jacquod, Phys. Rev. Lett. **98**, 164101 (2007).
[19] H. Kohler, H.-J. Sommers, S. Åberg, and T. Guhr, Phys. Rev. E **81**, 050103(R) (2010).
[20] E. P. Wigner, Ann. Math. **62**, 548 (1955); V. V. Flambaum, A. A. Gribakina, G. F. Gribakin, and M. G. Kozlov, Phys. Rev. A **50**, 267 (1994); Ph. Jacquod and D. L. Shepelyansky, Phys. Rev. Lett. **75**, 3501 (1995); J. L. Gruver, J. Aliaga, H. A. Cerdeira, P. A. Mello, and A. N. Proto, Phys. Rev. E **55**, 6370 (1997).
[21] M. C. Gutzwiller, *Chaos in Classical and Quantum Mechanics* (Springer, New York, 1990).
[22] J. Vanicek, Phys. Rev. E **73**, 046204 (2006).
[23] Ph. Jacquod, P. G. Silvestrov, and C. W. J. Beenakker, Phys. Rev. E **64**, 055203(R) (2001).